Extreme Mechanics Letters 61 (2023) 101999

Contents lists available at ScienceDirect

Extreme Mechanics Letters

journal homepage: www.elsevier.com/locate/eml

Electroadhesion zipping with soft grippers on curved objects

Massimiliano Mastrangelo [a], Fabio Caruso [a], Giuseppe Carbone [a], Vito Cacucciolo [a,b,*]

[a] Department of Mechanics, Mathematics and Management (DMMM), Politecnico di Bari, via E. Orabona 4, 70125 Bari, Italy
[b] Omnigrasp SRL, Via C. Rosalba 47/J, 70124 Bari, Italy

ARTICLE INFO

Article history:
Received 6 January 2023
Received in revised form 22 February 2023
Accepted 28 February 2023
Available online 9 March 2023

Keywords:
Electroadhesion
Soft grippers
Soft robotics
Zipping

ABSTRACT

Electroadhesion soft grippers generate extremely high holding forces (> 1 kg per gram of gripper) when the fingers wrap around the object. However, adding actuators on the soft fingers to close them on the object leads to increased stiffness, which reduces the roughness-scale conforming on the fingers to the object, resulting in lower adhesion forces. With the right materials and geometry, electroadhesion forces can alone drive a soft finger to zip on an object without any added actuator. By keeping the soft fingers free from any extra device, electroadhesion zipping combines macroscopic wrapping of fingers around an object with microscopic conforming of the finger's soft membrane to the object surface. Electroadhesion zipping shares the same mechanism with recently developed soft zipping actuators. Instead of two electrodes on polymer films zipping together and displacing a liquid, in Electroadhesion grippers the soft fingers, equipped with interdigitated electrodes, zip onto a curved object to grab it with high holding forces. In this work we investigate Electroadhesion zipping by reporting a model and a set of experimental data that relate the wrapping angle α with the applied voltage V, for given materials and geometry of object and soft fingers. We discovered that the phenomenon is governed by two voltage thresholds: a first one below which no zipping occurs (V no zip) and a second one above which the soft fingers fully collapse on the object (V full zip). We present analytical equations and design tools that quantify these voltage values for given bending stiffness, mass, shape, and capacitance of the soft finger–object pair. Our model shows that Electroadhesion zipping does not scale with V^2/d^2 (voltage squared over dielectric gap squared), as previously reported for Electroadhesion forces, but rather with V^2/d. Our experiments fit very well with the model results, especially when zipping on dielectric objects with non-tacky surfaces (e.g., paper). We demonstrate thin electroadhesive fingers that wrap around a wide set of objects made of different materials (from conductive to dielectric) and with different geometries, reaching wrapping angles up to 90°. The new design tools and experimental data will drive the design of electroadhesion soft grippers able to conform to nearly any shape and lifting objects heavier than 1000 times their own weight.

1. Introduction

Electroadhesion (EA) soft grippers [1–6] grasp fruit and vegetables without damaging them [7], separate textiles from a stack [8], are self-sensing [9] and hold large weights [10,11]. Electroadhesion is silent, clean and low-power. Thin, elastomer fingers conform to the shape of the object and ensure a delicate touch. EA creates mutual attraction between finger and object, which results in a large shear force [10–14] with negligible compression of the object. Effective grasping requires the fingers to wrap around the object, conforming to its shape and establishing large surface area contact. This wrapping can be achieved in two ways, (1) by an actuator, (2) using EA force. Adding actuators has the advantage of independent control yet results in stiffer fingers with reduced conformability and a complex fabrication [2–11]. Recent works by the authors show how optimizing the grasping posture of EA soft grippers can lead to over 1000x increased grasping force [7–12]. In this work, we focus on using EA forces to wrap the fingers around an object, combining high conformability, soft fingers, and large holding forces. Similar to electrostatic zipping actuators, EA fingers can be designed to spontaneously zip on an object when a voltage is applied. We report a model and a set of experiments that characterize the design parameters (mechanical and electrical) for the zipping to happen on objects with different materials and geometry. The achieved large wrapping angles promise very high forces with simple and compliant soft grippers.

Electroadhesion (EA) uses electric fields to generate normal and shear forces between two contacting surfaces [14]. It enables wall climbing robots [15], electro-haptic devices [16,17],

* Corresponding author at: Department of Mechanics, Mathematics and Management (DMMM), Politecnico di Bari, via E. Orabona 4, 70125 Bari, Italy.
E-mail address: vito.cacucciolo@poliba.it (V. Cacucciolo).

https://doi.org/10.1016/j.eml.2023.101999

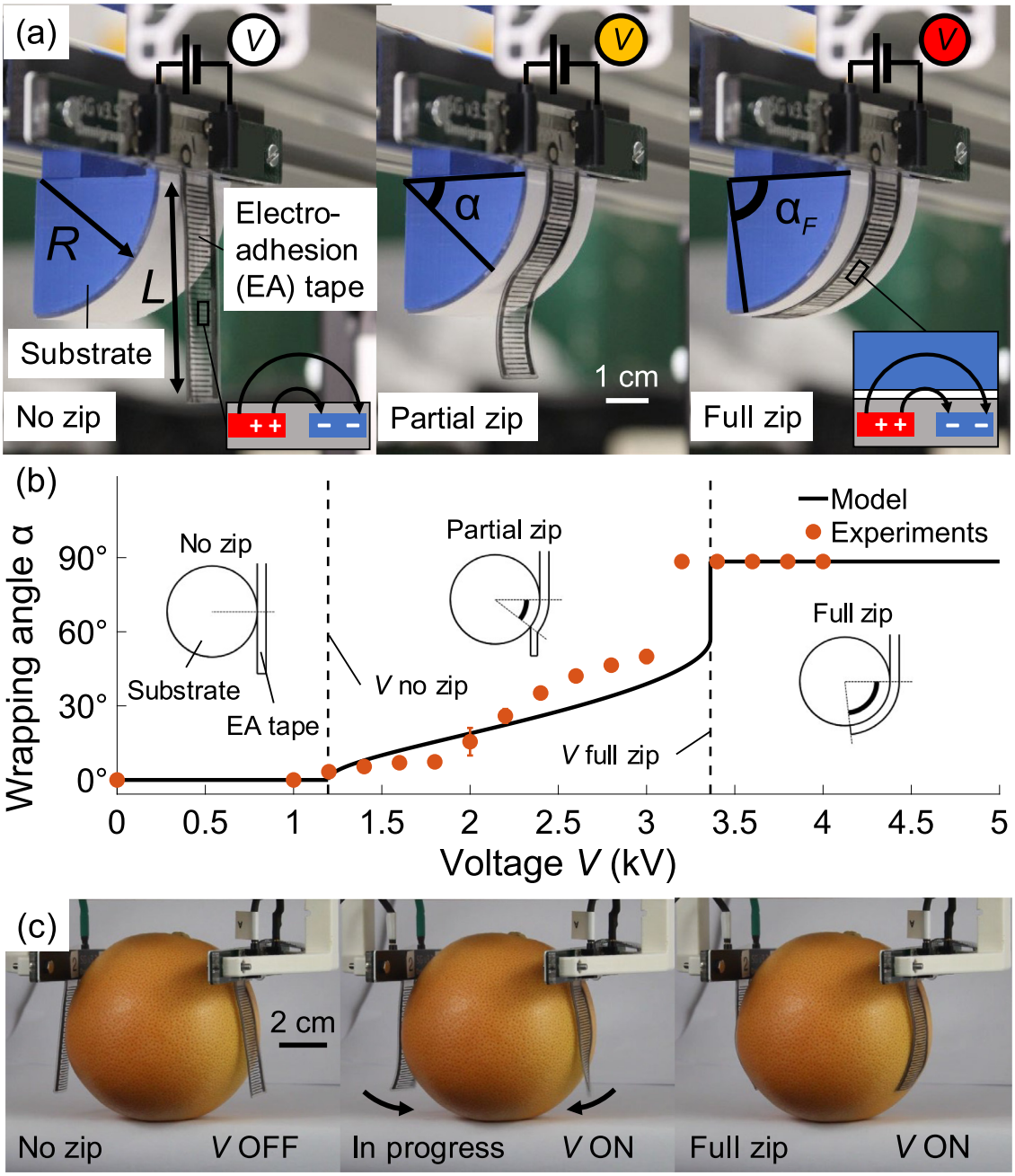

Fig. 1. (a) Zipping of an electroadhesion (EA) finger ($L = 48$ mm) on a cylindrical object ($R = 30$ mm), measured by the wrapping angle α. Applying a voltage difference V across the interdigitated electrodes of the EA finger creates electrostatic forces that attract the finger to the curved substrate. The higher the voltage, the higher the wrapping angle, until the finger completely zips onto the object (angle α_F). (b) Voltage — wrapping angle model and experimental results ($R = 30$ mm, DC voltage). Below the V no zip voltage threshold, the attraction forces are too weak to move the finger ($\alpha = 0$). When the voltage exceeds V no zip, the finger partially zips on the object ($\alpha < \alpha_F$). When the voltage further exceeds the V full zip threshold, the finger fully zips on the object, similarly to a pull-in instability ($\alpha = \alpha_F$). (c) A soft gripper with two fingers that wraps around a grapefruit using electroadhesion zipping (EAZ).

soft actuators (where EA induces muscle-like contraction of the device) [18–20], electrical wound patches [21], and grippers [2–4]. Its advantages are electrical control, absence of residues, and adaptation to a wide range of shapes and materials. EA soft grippers use interdigitated electrodes buried in a dielectric elastomer. When a voltage is applied between the electrodes, the fringing electric field induces charges on both the surface of the finger and the object. The surfaces mutually attract, generating adhesion (Fig. 1a).

The holding force of EA grippers is strongly influenced by the grasping posture. As shown in previous works by the authors, the holding force increases by several orders of magnitude when the peeling angle between finger and object decreases [7] and keeps increasing exponentially when the fingers wrap around the object [10,12]. Grippers that actively conform to the objects' shape have been demonstrated by combining EA with Dielectric Elastomer Actuators (DEAs) [2], Fin-Ray mechanism [22], and pneumatic actuation [13]. While helping the fingers envelop the object macroscopically, adding actuators results in higher stiffness, which negatively influences the actual contact area between the gripper and the object at small scale. In contrast, EA zipping leverages electrostatic forces to wrap the fingers around the object without added stiffness, maximizing conformability at the roughness length scale. Electrostatic zipping has recently been

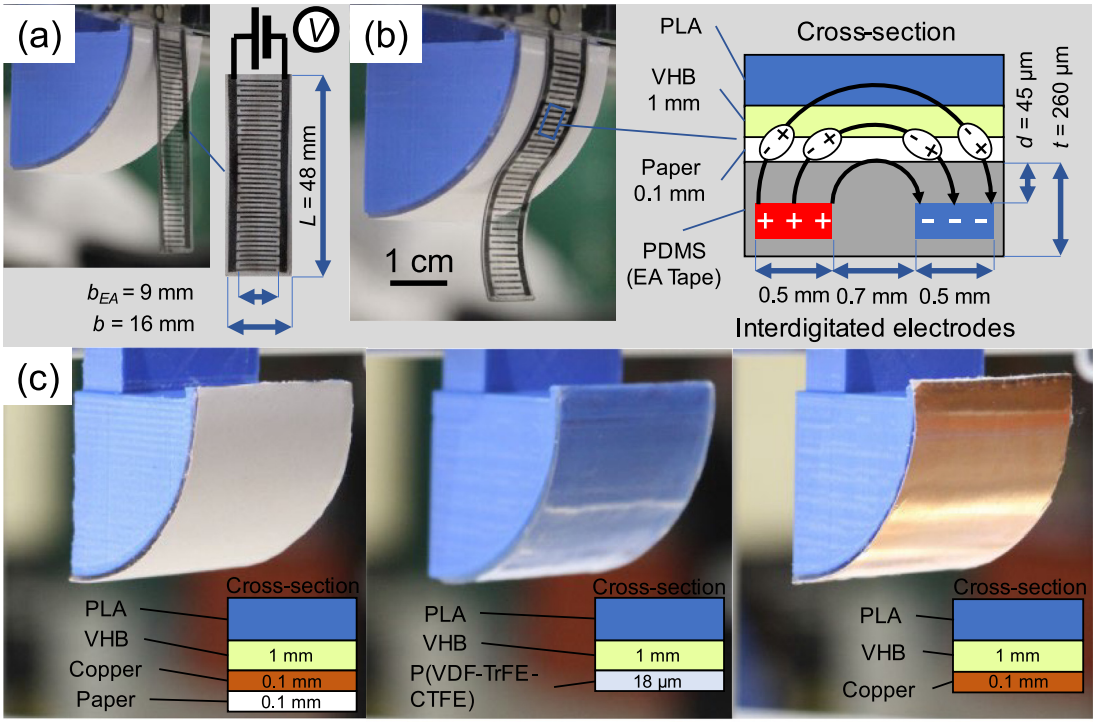

Fig. 2. (a) EA finger starting position for the experiments: the finger is vertical, tangent to the object. The finger length is $L = 48$ mm. $b = 16$ mm is the finger width, and $b_{EA} = 9$ mm is the width of the interdigitated electrodes region. (b) Finger partially zipped over the paper-covered object and schematic cross-section of the finger. The presence of the finger induces charges onto the object's surface, and the finger and the object mutually attract. (c) Pictures of the curved objects used in the experiments covered by: 0.1 mm thick paper on top of 0.1 mm-thick copper (left); 18 µm-thick P(VDF-TrFE-CTFE) (center); 0.1 mm-thick copper (right).

demonstrated in a wide range of high-performance actuators, such as electro-ribbon [18], HASELs [19], and HAXELs [20]. In these devices the zipping typically happens between two films, each containing a flat electrode. Dielectric liquids are placed in-between the films to amplify the force output. EA zipping shares the main mechanism with zipping actuators but concerns soft fingers with interdigitated electrodes that zip on a curved object. There is no liquid in this case and the object can be made of any material and does not include electrodes. The goal is to use EA forces to make the fingers wrap around the object, which leads to very high grasping forces. Wrapping requires the fingers to bend and lift their center of mass (Fig. 1a). The wrapping angle that can be achieved depends on the ratio between the EA forces and the mechanical restoring forces (bending moment and weight).

This work reports an analytical and experimental investigation of EA zipping on curved objects. Our model and experimental data quantify the relation between the maximum wrapping angle, the applied voltage and the finger and object mechanical (bending stiffness, mass, object radius) and electrical (dielectric constant) parameters. We discovered that the zipping of a flat finger on a cylindrical object is characterized by two voltage thresholds: a first one under which no zipping occurs and a second one over which the whole finger collapses onto the object (Fig. 1b). Our results show that the zipping angle increases with V^2/d, unlike the V^2/d^2 dependence previously reported for EA forces. By characterizing the two voltage thresholds we aim at providing a design tool to select materials and geometry for EA soft grippers that zip and effectively grasp a wide range of objects. We finally demonstrate the successful zipping of a pair of soft EA fingers on a set of objects (Fig. 1c and Video 4).

2. Materials and methods

We conducted zipping tests with EA fingers on cylindrical objects to measure the wrapping angle α while varying the applied voltage V. We tested both the quasi-static and dynamic responses. We tested both zipping and unzipping to evaluate the hysteresis.

We used objects with radii of 30 and 45 mm, coated with either dielectric or conductive materials. As EA fingers we used thin rectangular stripes (48 mm long, 16 mm wide, 0.26 mm thick) made of PDMS (Polydimethylsiloxane) with carbon-loaded PDMS electrodes (Fig. 2a). The electrodes are interdigitated, with an electrode width of 0.5 mm and a pitch of 0.7 mm (Fig. 2b). The thickness of the insulating PDMS layer between electrodes and object is 0.045 mm. Since the volume fraction of electrodes materials is small, we assume homogeneous material properties equal to those of PDMS Sylgard 184 (Dow Corning): Young's modulus $E = 3.9$ Mpa [23], density $\rho = 1030$ kg/m^3 (Dow Corning datasheet [24]).

We used Ketjenblack EC-300J (AkzoNobel) as carbon black for the electrodes. Finger fabrication followed the procedure described in [7]: (1) blade casting and curing of the PDMS backing, (2) blade casting and curing of conductive PDMS-carbon composite, (3) laser engraving of the electrodes, (4) blade casting and curing of PDMS top insulating layer.

We used 3D-printed PLA (Polylactic Acid, dielectric constant $\varepsilon_{PLA} = 3$ [25]) for the structure of the cylindrical objects (Fig. 2). We applied four different coatings on these objects to study the influence of electrical and surface properties (Fig. 2c): (1) 0.1 mm-thick paper ($\varepsilon_{paper} = 3$ [26]), (2) 0.1 mm-thick paper on top of 0.1 mm-thick copper, (3) 18 µm-thick P(VDF-TrFE-CTFE) ($\varepsilon_{PVDF} = 30$, PolyK Technologies [27]), (4) 0.1 mm-thick copper. Coatings are bonded to the PLA object using a 3M VHB 4910 adhesive (1 mm-thick, dielectric constant $\varepsilon_{VHB} = 4.7$ [28]).

Each experiment starts with the finger in vertical position, tangent to the object (Fig. 2a). We apply the voltage at the electrodes and measure the wrapping angle α. For the quasi-static tests, we increased the voltage at a slow rate (200 V every 10 s) until full zipping. For the dynamic experiments, we applied a voltage step for 3 s, followed by voltage off for 3 s. This cycle is

repeated increasing the voltage value by 400 V. We used voltage values not exceeding 4 kV to prevent electrical breakdown (4 kV corresponds to an electric field value in the top insulating layer of about 45 kV/mm, well below the 100 kV/mm breakdown threshold of Sylgard 184 films [29]). We used both DC and AC voltage (10 Hz bipolar square wave) applied with a DC-HVDC converter (XP Power A series) and high-voltage optocouplers (VMI OC 100G).

3. Theory

This section describes the mathematical model relating the wrapping of the EA finger, described by the angle α, with the applied voltage V, for given materials and geometries of EA finger and object. We derived the formulation by writing the potential energy balance (in differential form) of the system composed of finger + object + battery, as similarly done for dielectric elastomers [30,31] and fluid transducers [32,33]. The model identifies two voltage thresholds. First, when the voltage is below a minimum value ($V < V_{NO\,ZIP}$) the EA finger does not move ($\alpha = 0$). For $V > V_{NO\,ZIP}$ the wrapping angle α increases with the voltage. When the voltage exceeds the second threshold ($V > V_{FULL\,ZIP}$) the finger fully wraps around the object, reaching maximum angle $\alpha_F = L/R$, with L the finger length and R the object radius (assumed constant). The relation between angle and voltage is nonlinear due to the gravitational energy term, while the electrostatic and the elastic energy terms are linear in this configuration.

We also report the equations of equilibrium obtained by writing the total potential energy of the system (function of α and V) and identifying the points where its derivative with respect to the angle α is zero. This second method is described in Supplementary Section S1. The two methods lead to the same results.

3.1. Model formulation

We consider the system composed of the EA finger, modeled as an electrical capacitor formed by the interdigitated electrodes, air, and the curved object in its proximity, and a power supply modeled as a battery providing constant voltage V. The energies involved in the wrapping process are (1) the bending strain energy of the finger (Fig. 1a) and (2) the gravitational energy of the finger (Fig. 1b), and (3) the electrical energy (Fig. 1c) of both the finger capacitor and the battery. The model is quasi-static, so we do not include dynamic terms.

We analyze the equilibrium of the EA finger zipping on a cylindrical object of radius R. To write the equilibrium equation, we consider a small perturbation dα from the system equilibrium described by the wrapping angle α and the voltage V. A change in wrapping angle dα is associated with the following variations in the system (Fig. 3d, e): (1) the length of the EA finger in contact with the object increases linearly by a quantity dαR, resulting in an increased capacitance of the EA capacitor, (2) a finger section of length dαR deforms elastically from an undeformed straight position into a bent position of radius R, (3) the center of mass of the EA finger is lifted vertically by a quantity dz (nonlinear function of α). The energy required for an infinitesimal increase of (1) the electrostatic energy stored in the capacitor dU_{EL}, (2) the bending strain energy dU_F and (3) the gravitational energy dU_G of the EA finger is provided by the electrical power supply in the form of electrical work $dW_{EL} = dQV$. The potential energy balance of the system at equilibrium is written in differential form as:

$$dU_{EL} + dU_F + dU_G = dW_{EL} \tag{1}$$

The electrostatic energy of the capacitor can be written as $dU_{EL} = 1/2dQV$, with Q the charge stored in the capacitor. The total electrical energy variation of the system results in $dU_{EL} - dW_{EL} = -1/2dQV$. We introduce $dU_{EA} = 1/2dQV = 1/2dC\,V^2$ as the variation of the electroadhesion energy of the system (with C the EA finger capacitance), where the electroadhesion energy is the electrical energy stored in the finger capacitor. Eq. (1) can be then written as

$$dU_F + dU_G = dU_{EA} \tag{2}$$

showing that the increased EA capacitive energy associated with an increase in the wrapping angle dα balances the increase in mechanical energy $dU_F + dU_G$.

3.2. Gravitational energy

When the wrapping angle increases by a quantity dα, a finger portion of length Rdα zips on the object (Fig. 3d) and its center of mass rises by a quantity $1/2R$d$\alpha\,(1 - cos\alpha)$ (Fig. 3e). The mass of this finger portion is Rd$\alpha\rho tb$, with ρ, t and b the mass density, thickness, and width of the finger, respectively. The center of mass of the remaining unzipped portion of the finger rises by a length Rd$\alpha\,(1 - cos\alpha)$. The mass of this unzipped portion is $(L - (\alpha + d\alpha)\,R)\,\rho tb$. The infinitesimal variation of the gravitational energy dU_G is

$$\begin{aligned} dU_G = {} & 1/2R\mathrm{d}\alpha\,\rho tbgR\mathrm{d}\alpha\,(1 - cos\alpha) \\ & + (L - (\alpha + d\alpha)\,R)\,\rho tbgR\mathrm{d}\alpha\,(1 - cos\alpha) \end{aligned} \tag{3}$$

The derivative of U_G with respect to α results in (second order terms neglected)

$$\frac{dU_G}{d\alpha} = (L - \alpha R)\,\rho tbgR\,(1 - cos\alpha)\,, \tag{4}$$

which is nonlinear due to the $cos\alpha$ term.

3.3. Bending strain energy

When the finger zipping increases of an angle $d\alpha$, a finger length Rdα bends from straight to circular (radius R), generating the restoring moment M (Fig. 3e). The associated bending strain energy is $dU_F = \frac{1}{2}M d\alpha = \frac{1}{2}\frac{EI_x}{R}d\alpha$, according to the Euler–Bernoulli slender beam theory, with E = finger Young's modulus, $I_x = \frac{bt^3}{12}$ second moment of area of the finger (Supplementary figure 1a). The infinitesimal variation in the bending strain energy of the finger is $dU_F = \frac{1}{24}\frac{Ebt^3}{R}d\alpha$, so the derivative of U_F respect to α is a constant value

$$\frac{dU_F}{d\alpha} = \frac{1}{24}\frac{Ebt^3}{R} \tag{5}$$

3.4. Electroadhesion energy

We define $C(\alpha)$ the finger capacitance at wrapping angle α. C_c is the capacitance of the finger when fully in contact with the object ($\alpha = \alpha_F$), and C_∞ is the capacitance when the whole finger is at an infinite distance from the object. When the wrapping angle α increases, the capacitance of the finger $C(\alpha)$ increases since the dielectric constant of the object is always higher than the one of air. To capture the increase in capacitance due to an infinitesimal zipping $d\alpha$, we introduce the capacitance variation per unit length $\Delta\hat{c}$. $\Delta\hat{c}$ is defined as the difference between the capacitance of a semi-electrode pair (half positive and half negative electrode, separated by a distance w, Fig. 3c) when in contact with the object and when at infinite distance, divided by its length. When the finger zips of an angle $d\alpha$, its capacitance increases by a quantity $\Delta\hat{c}R$dα.

We use a semi-electrode pair as a unit since it fully captures the electric field shape for interdigitated electrodes. We computed the capacitance of a semi-electrode pair by using COMSOL

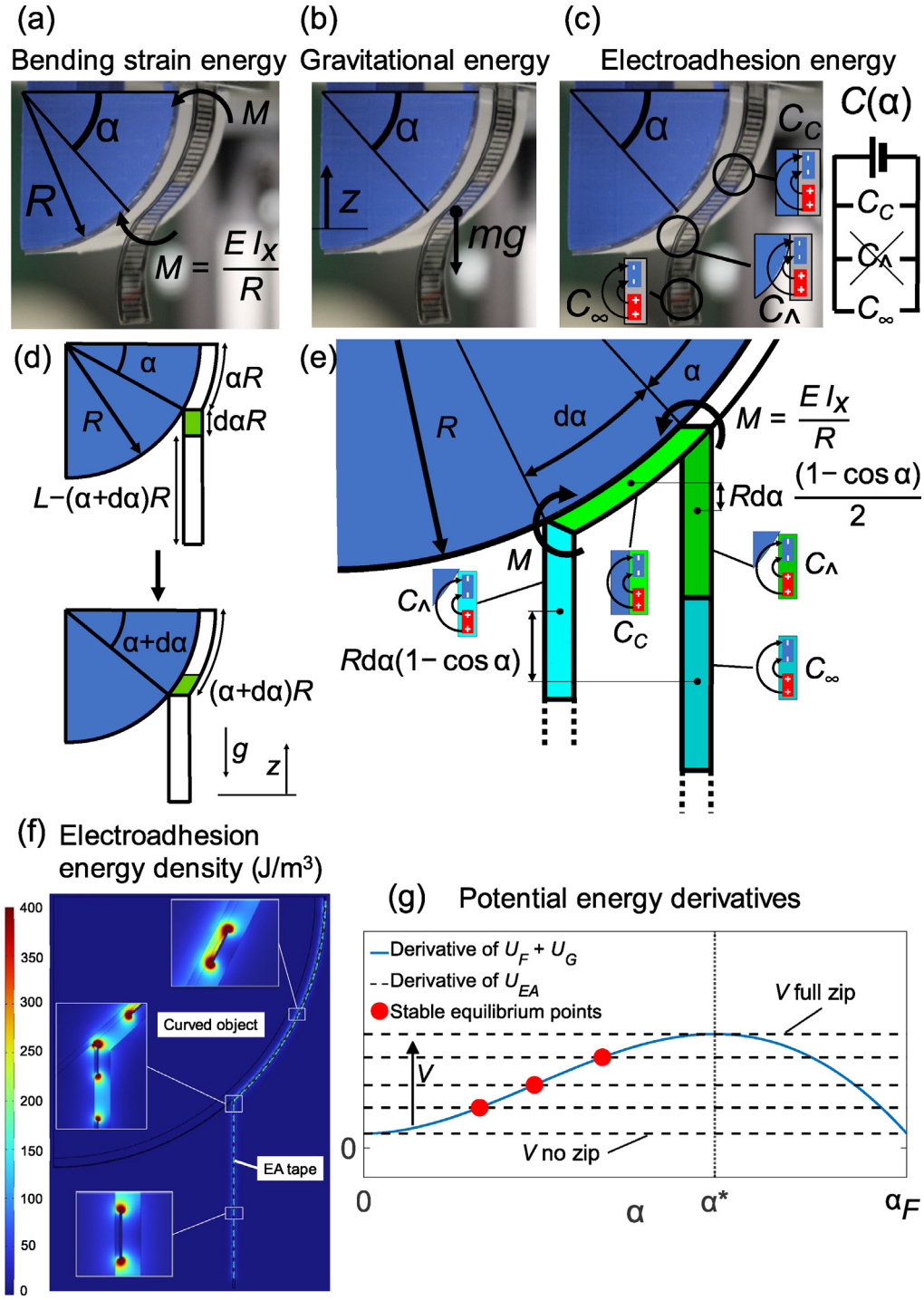

Fig. 3. (a, b, c) the energy components of the system involved in the zipping process: (a) the bending strain energy, due to the bending of the finger around the object. $M = EI_x/R$ is the pure homogeneous moment due to conforming to the constant curvature $1/R$ of the object according to the Euler–Bernoulli slender beam theory, with E = finger Young's modulus, $I_x = bt^3/12$ = second moment of area of the finger section; (b) the gravitational energy due to the lifting of the finger center of mass (m); (c) the electroadhesion energy of the capacitor formed by the object, the finger and the surrounding air. The capacitance of the system $C(\alpha)$ is calculated based on the capacitance values when the finger is fully zipped (C_c) or at infinite distance from the object (C_∞). We found that the proximity of the object (accounted by $C_\wedge$) barely affects the capacitance of the system. (d) The zipping advancement by an angle $d\alpha$ involves the wrapping of an infinitesimal section $Rd\alpha$ of the finger. (e) When the infinitesimal section $Rd\alpha$ of the finger wraps the object, it bends, and stores strain energy related to the moment $M = EI_x/R$. Its center of mass rises by a quantity $(Rd\alpha/2)(1 - cos\alpha)$, and the remaining unzipped finger center of mass rises by $Rd\alpha\,(1 - cos\alpha)$. The capacitances of both the contributes change accordingly to new positions assumed with respect to the object. (f) Electrostatic energy density distribution of the finger shows a peculiar distribution at the zipping boundary, but as shown by (g) it does not strongly affect the capacitance of the system. (g) Potential energy derivatives (Eq. (8)). The electroadhesion term increases with the applied voltage. Red points in the graph are the stable equilibrium points of the system. No equilibrium is possible until the voltage reaches the V no zip value. Stable equilibrium proceeds toward higher wrapping angles with increasing voltage, until full wrapping is reached. (For interpretation of the references to color in this figure legend, the reader is referred to the web version of this article.)

FEM electrostatic simulations as done in [7], since for interdigitated geometries we cannot use simple analytical formulas as for parallel plate capacitors. By introducing $\Delta\hat{c}$ and computing it once for given geometry and materials using FEM simulations, we can then use an analytical formulation similar to parallel plate capacitors, where capacitance increases linearly with capacitor length $C(\alpha) = \Delta\hat{c}R\alpha$. In reality the unzipped portion of the finger is at a finite distance from the object (Fig. 3e), but we show that (1) we can neglect the small field concentration at the zipping boundary since this boundary effect is constant with zipping (the zipping boundary translates) and so it does not influence the capacitance difference and (2) the electrostatic energy of an unzipped region a few mm away from the object is practically very similar to the one of a finger at infinite distance (Fig. 3f and Fig. S2). demonstrates that these approximations introduce a negligible error, by comparing the capacitance computed as $C(\alpha) = \Delta\hat{c}R\alpha$ and the one obtained simulating the whole finger using COMSOL FEM. Following these considerations, we obtain the variation of U_{EA} with α as a constant value during zipping, depending on voltage squared

$$\frac{dU_{EA}}{d\alpha} = \frac{C_c - C_\infty}{2L}RV^2 = \frac{1}{2}\Delta\hat{c}RV^2 \tag{6}$$

3.5. Wrapping angle as a function of the applied voltage

Following the potential energy balance of the system (2), we can write the equilibrium as

$$\frac{d(U_G + U_F)}{d\alpha} = \frac{dU_{EA}}{d\alpha}, \tag{7}$$

and by using Eqs. (4)–(6) we obtain:

$$(L - \alpha R)\,\rho tbgR\,(1 - cos\alpha) + \frac{1}{24}\frac{Ebt^3}{R} = \frac{1}{2}\Delta\hat{c}RV^2 \tag{8}$$

The LHS and RHS of Eq. (8) are plotted in Fig. 3g. The intersection points in the plot represent the states of equilibrium. The RHS (EA bending moment) increases with V^2 and is plotted for different values of V. No equilibrium point exists until $\frac{dU_{EA}}{d\alpha}$ reaches a minimum value, showing that zipping does not start until a voltage threshold (V no zip) is reached. The value of V no zip can be calculated by using Eq. (8) at $\alpha = 0$

$$V_{NO\ ZIP} = \frac{1}{R}\sqrt{\frac{1}{12}\frac{Ebt^3}{\Delta\hat{c}}}. \tag{9}$$

It is interesting to notice that the mass density disappears (mass does not influence V no zip). Eq. (9) quantifies the minimum voltage that needs to be applied to an EA finger to initiate the zipping process. A higher bending stiffness leads to a higher $V_{NO\ ZIP}$ and a higher $\Delta\hat{c}$ leads to a lower value. Zipping on objects with smaller radius R requires a higher voltage.
Solving (8) for the voltage, we obtain the relationship between applied voltage and wrapping angle at equilibrium

$$V = \sqrt{\frac{2}{\Delta\hat{c}}\left[\left(\frac{L}{R} - \alpha\right)\rho tbgR\,(1 - cos\alpha) + \frac{1}{24}\frac{Ebt^3}{R^2}\right]} \tag{10}$$

A higher wrapping angle α requires a higher voltage V. Stable equilibrium (red points in Fig. 3g) at intermediate wrapping angle $\alpha < \alpha_F$ are only possible until a certain angle α^*. Beyond that point, the whole finger collapses onto the object, similarly to an electrostatic pull-in. This effect is due to the nonlinear form of the gravitational energy term. The voltage that corresponds to this threshold is defined as V full zip. We compute its value using (8) and replacing $\alpha = \alpha^*$. The angle α^* is obtained using the stability condition $\frac{d^2(U_G+U_F)}{d\alpha^2} = \frac{d^2U_{EA}}{d\alpha^2}$, that gives:

$$\rho tbgR[(L - \alpha R)sin(\alpha) + Rcos(\alpha) - R] = 0. \tag{11}$$

Eq. (11) is satisfied for $\alpha = 0$ and $\alpha = \alpha^*$. By rearranging and by recalling $\alpha_F = L/R$, one gets, for the case $\alpha = \alpha^*$:

$$\alpha_F = \alpha^* + \frac{1 - cos(\alpha^*)}{sin(\alpha^*)}. \tag{12}$$

The relationship between α_F and α^* appears to be constant and independent of any physical parameters. The reason is that both the bending strain energy and the EA energy are linear with α, so they disappear in the second derivative. Therefore, α^* depends only on the shape of the gravitational energy function and its geometric nonlinearities. We solved Eq. (12) numerically for $\alpha_F < 90°$ and found that α^* can always be approximated as $\alpha^* = 0.65\alpha_F$. This result means that the angle at which the instability occurs is always the 65% of the final zipping angle $\alpha_F = L/R$. By using $\alpha = \alpha^* = 0.65\alpha_F$. in (10) we get an analytical solution for V full zip (valid for $\alpha_F < 90°$, which is practically always the case for EA soft grippers)

$$V_{FULL\ ZIP} = \sqrt{\frac{2}{\Delta\hat{c}}\left[0.35\rho btLg\left(1 - cos(0.65\frac{L}{R})\right) + \frac{1}{24}\frac{Ebt^3}{R^2}\right]}. \tag{13}$$

Eqs. (9) and (13) can be rewritten to show the dependence of the two voltage thresholds on the ratio between the physical parameters of the system. By defining $BS = \frac{1}{12}Ebt^3$ as the bending stiffness of the EA finger, Eq. (9) becomes:

$$V_{NO\ ZIP} = \frac{1}{R}\sqrt{\frac{BS}{\Delta\hat{c}}}. \tag{14}$$

$V_{NO\ ZIP}$ represents both the theoretical threshold to initiate zipping and to initiate unzipping (Fig. 3g).
Similarly, by defining $\gamma = 0.70R^2\left(1 - cos(0.65\frac{L}{R})\right)$ the geometric factor, and using the mass $m = \rho btL$, V full zip from Eq. (9) becomes:

$$V_{FULL\ ZIP} = \frac{1}{R}\sqrt{\frac{mg\gamma + BS}{\Delta\hat{c}}}. \tag{15}$$

Eqs. (14) and (15) can be used to quantify the zipping voltage required to initiate and fully zip an EA soft finger on a cylindrical object, given geometry and materials of both finger and object.

3.6. Improving zipping performance by maximizing the change in capacitance $\Delta\hat{c}$

In this section we report a set of simulations that map the change in capacitance $\Delta\hat{c}$ for given thickness d of dielectric layer that separates the electrodes from the object and spacing w of the interdigitated electrodes. These results can be used as a design tool to increase $\Delta\hat{c}$ and decrease the voltage required for zipping, for given mass and bending stiffness of the EA fingers.

The analytical model derived in the previous section describes how the zipping process is influenced by four quantities: (1) finger bending stiffness BS, (2) finger mass m, (3) capacitance variation per unit length $\Delta\hat{c}$; (4) a geometric factor γ. Eqs. (14) and (15) suggest that the voltage required to start zipping (V no zip) and reach full wrapping on the object (V full zip) can be reduced by increasing the change in capacitance per unit length $\Delta\hat{c}$, defined as the difference between the capacitance of a semi-electrode pair when in contact with the object C_c and when at infinite distance C_∞, divided by its length.

As described in the previous section, we used COMSOL Multiphysics to compute the values of C_c and C_∞ for given geometry and materials, since the interdigitated electrodes geometry prevents the use of simple analytical formulas. The electrodes were modeled as contours with length 250 μm, height 25 μm, and an

out-of-plane dimension of 9 mm, with rounded edges to avoid field singularities. These values were chosen equal to the ones of the real finger used in the experiments. A constant potential difference V was applied between the electrodes. The EA finger cross section is a rectangle with a fixed height of 260 μm and a length that was varied as a function of the spacing between the electrodes w. The presence of the object (top) and the air (bottom) was modeled with a sufficiently large bounding box (height 3 mm) to ensure that the size of the boundaries does not influence the estimated capacitance. Finally, to take into account the different dielectric materials involved, a dielectric permittivity was assigned to air ($\varepsilon_{air} = 1$), object (ε_{object}) and finger (ε_{tape}). Fig. 4a shows a schematic representation of the semi-electrode pair used in the simulations.

Fig. 4b–d show the capacitance variation $\Delta\hat{c}$ as a function of the ratio between the spacing between the electrodes and the thickness of the dielectric layers w/d, with $d = 45$ μm, for different combinations of dielectric permittivity of object and EA finger. All plots show the same trend. The change in capacitance per unit length $\Delta\hat{c}$ increases by decreasing w/d, which is a result of the increase in the electrostatic energy density due to the reduction of the spacing between the electrodes (in other words, same electrodes boundaries per unit length). Values of $w/d < 2$ are not shown as such geometry results in higher electric field in-between the electrodes than between electrodes and object. Such situation is unwanted as the electric field in-between the electrodes does not contribute to EA. Fig. 4b shows that when ε_{tape} is small, increasing ε_{object} leads to higher $\Delta\hat{c}$. Fig. 4c, d show that increasing ε_{tape} leads to a higher $\Delta\hat{c}$ only until $\varepsilon_{tape} \leq \varepsilon_{object}$. When $\varepsilon_{tape} \geq \varepsilon_{object}$, further increasing ε_{tape} has negligible advantages. This effect can be explained by considering that the increase in ε_{tape} leads to an increase in both C_c and C_∞, while ε_{object} influences only C_c.

Finally, we produced two maps that can be used as design tools for EA soft grippers. Fig. 4e,f show the voltage required to initiate zipping (V no zip) and the voltage for fully wrapping the fingers around the object (V full zip) for different values of the dielectric layer thickness d, of the fingers bending stiffness BS and of the fingers mass m. We kept constant the ratio $w/d = 16$ (value used in our experiments), the dielectric permittivity of the finger ($\varepsilon_{tape} = 3$) and the object ($\varepsilon_{object} = 3$). The plots are obtained by first computing $\Delta\hat{c}$ using COMSOL and then using this value in Eq. (14) and 15 to compute V no zip and V full zip for given mass and bending stiffness and with the geometrical factor $\gamma = 311$ mm^2, which corresponds to an object radius of 30 mm and a finger length of 48 mm. Figs. 4e and 4f show the regions of feasible design to obtain zipping with given finger geometry and material. As previously discussed, EA zipping does not scale with V^2/d^2. On the contrary, higher dielectric thickness d and higher voltage lead to successful zipping with increased bending stiffness and mass. This effect will in turn influence the holding force of EA grippers, for two reasons. The first one is that zipping influences how much a finger macroscopically wraps around an object, which greatly influences the grasping force [1]. The second reason is that zipping governs the microscopic compliance of the gripper with an uneven surface, which determines the surface area of the contact, which in turns determines the adhesion force [2].

4. Results and discussion

This section reports the results of the zipping experiments with EA fingers and the comparison with the model predictions. We conducted the following tests: quasi-static zipping tests with different object radii using AC (a) and DC (b) voltage, cycling zipping and unzipping tests (c), comparison between different coating materials (d), dynamic zipping tests (e), load lifting (f).

For all the quasi-static tests the voltage rate is 200 V every 10 s. For AC voltage we use a superimposed bipolar square wave at 10 Hz. Each test is repeated three times and we plot mean and standard deviation over the three trials.

Fig. 5a and Supplementary video 1 show the validation of the zipping model, at two different radii (30 and 45 mm). Voltage is applied from 0 to 3.8 kV using a superimposed AC bipolar square wave (10 Hz). The AC modulation has the effect of both reducing dry adhesion and preventing charges building up in the dielectric materials facing the electrodes. Both model and data show that until reaching a minimum voltage value V no zip, the finger does not start moving. For higher voltages, the EA finger partially zips (wrapping angle $\alpha > 0°$) and keeps this position as long as the voltage is held. When the voltage value exceeds the V full zip threshold, the EA finger fully zips on the object. The model fits the trend in the data with good accuracy, especially considering that no fitting has been done on the parameters (all physical values). Possible reasons for the observed discrepancies include: (1) non-flatness of the EA finger due to the fabrication process, (2) unzipped region modeled as a vertical straight line for simplicity.

Fig. 5b repeats the configuration of Fig. 5a (the model is identical) but with the use of DC voltage. We observe that DC voltage leads to zipping at a lower voltage compared with model predictions. This effect is arguably due to charges building up in the dielectrics with time, as described in literature for EA and other electrostatic actuators [17].

Fig. 5c and Supplementary video 2 present model and experimental results for a zipping and unzipping cycle, using both DC and AC voltage. Due to the nonlinear shape of the system free energy (see Supplementary figure 1c) the EA finger remains zipped on the object when the voltage is decreased below the V full zip value. This effect is captured by the model and reflected in both AC and DC experiments. The model prediction is that unzipping should happen for $V \leq V$no zip. However, the unzipping with AC voltage happens earlier (higher voltage) than model predictions. The reason lies in the flatness of the free energy function in the full zip configuration (the range of stability is narrow). Dynamic effects due to AC oscillations are large enough to induce earlier detachment. In the DC case on the contrary, the finger remains attached even when voltage is removed (no unzip), arguably due to building up of charges in the dielectrics and creation of dry adhesion forces due to prolonged electrostatic pressure.

To account for materials with different surface and electrical properties, we measured both no zip and full zip voltage values on a 30 mm radius object with 4 different coatings (quasi-static, DC voltage) (Fig. 5d). Coating materials: 0.1 mm-thick copper, 0.1 mm-thick paper on top of 0.1 mm-thick copper, 18 μm-thick P(VDF-TrFE-CTFE), 0.1 mm-thick paper, all bonded to the object by means of 1 mm-thick VHB. Paper was chosen for most experiments as in normal conditions it does not stick to the silicone of the EA finger (negligible dry adhesion). We observe very good agreement between model and experiments for the case of paper. We then tested 18 μm-thick P(VDF-TrFE-CTFE), which is a high-k material (dielectric constant $\varepsilon = 30$ [27]). The model predicts lower values for both V no zip and V full zip compared to paper as the higher ε leads to higher electrostatic forces. Data also show earlier zipping, while the value of V full zip is over 40% higher than model predictions. The reason behind this difference is yet to be understood. Possible explanations lie in the polarization dynamics of P(VDF-TrFE-CTFE). Since EA works with both dielectric and conductive objects, we also tested with an electrically conductive surface (0.1 mm-thick copper coating). In this case both V no zip and V full zip predicted by the model are even lower than the $\varepsilon = 30$ case, as electrostatic forces are even higher. However, data values are over two times higher than predictions, and only slightly lower than data for paper

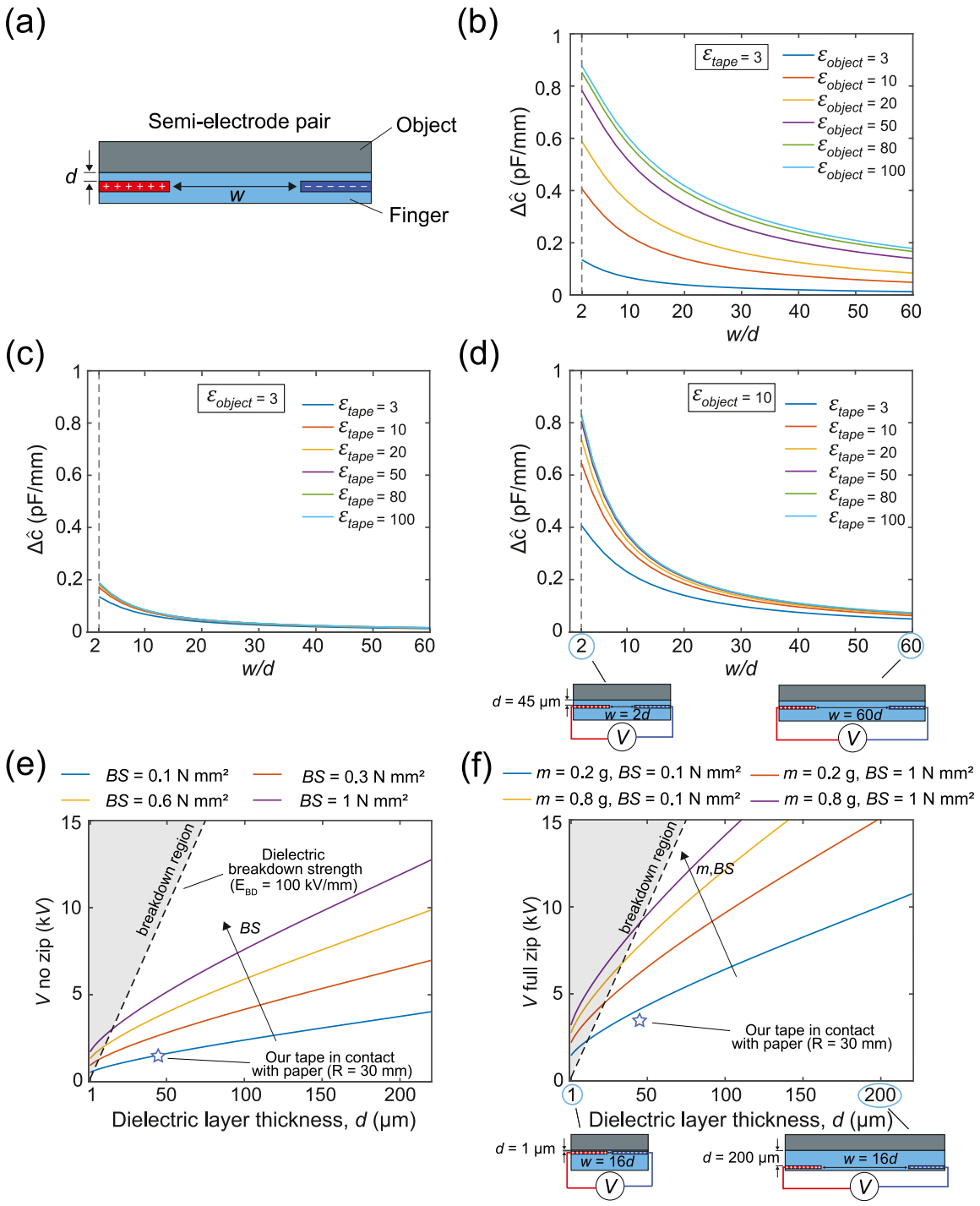

Fig. 4. Influence of dielectric layers thickness and spacing between the electrodes on the zipping performance of an EA finger. (a) Schematic representation of the semi-electrode pair used in COMSOL Multiphysics to estimate the capacitance variation per unit length $\Delta\hat{c}$, which influences the zipping voltage (see Eqs. (14) and (15)). (b) Capacitance variation as a function of the ratio w/d for different values of ε_{object}. Lower values of w/d lead to an increase in $\Delta\hat{c}$. (c) Capacitance variation as a function of the ratio w/d for different values of ε_{tape}. ε_{tape} has little influence on $\Delta\hat{c}$ when the dielectric permittivity of the object is small $\varepsilon_{object} = 3$. (d) Capacitance variation as a function of the ratio w/d for different values of ε_{tape}, with $\varepsilon_{object} = 10$. Increasing ε_{tape} leads to higher $\Delta\hat{c}$ only when $\varepsilon_{tape} \leq \varepsilon_{object}$. (e) Design tool showing V no zip as a function of dielectric layer thickness and fingers bending stiffness, highlighting feasible and unfeasible (breakdown) zipping regions. f) Design tool for V full zip, showing feasible and unfeasible design regions with given dielectric layer thickness, mass and bending stiffness of the EA finger.

coating. We cannot draw a conclusion about this discrepancy with these data only: the model does not include dynamics of electrical charges and by changing coating, both electrical and surface properties change at the same time. In order to control for surface, we finally tested with an object coated by 0.1 mm-thick paper on top of 0.1 mm-thick copper. In this configuration, electrical forces are higher than in the paper case (due to the copper layer), yet the surface is unchanged. The error between

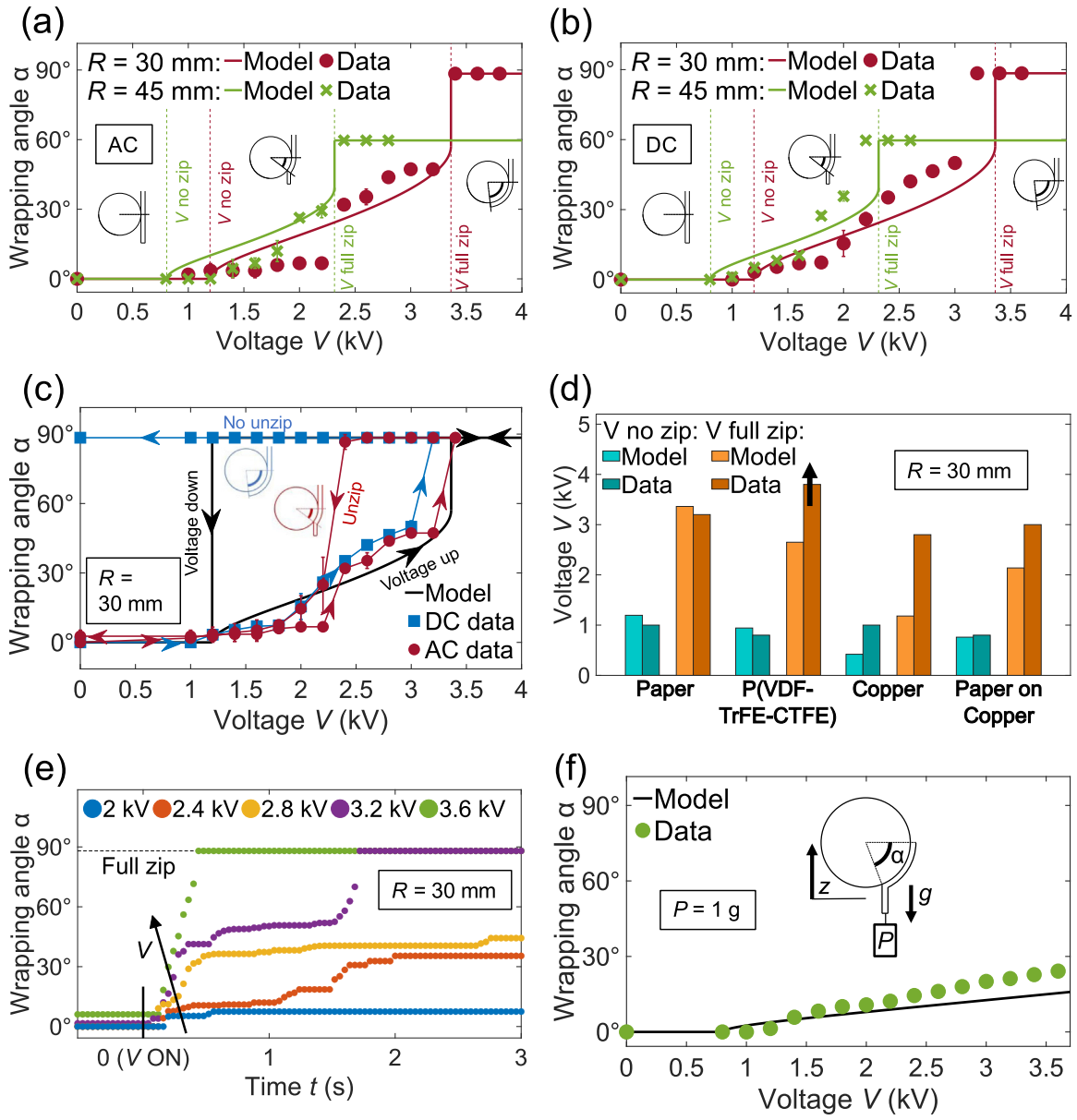

Fig. 5. (a, b) Validation of the zipping model for two different object's radii (30 and 45 mm), by applying increasing AC (a) and DC (b) voltages. Both cases show the absence of wrapping until a voltage value (V no zip) is applied, and the increase in the wrapping angle with the voltage until full zip. (c) Zipping and unzipping cycle for both AC and DC voltage ($R = 30$ mm). Apart from differences between the two cases, the experiments capture the hysteresis predicted by the model due to the nonlinear shape of the potential energy. (d) Comparison between model outcomes and experimental results of the wrapping of the EA finger around various curved substrates ($R = 30$ mm). The theoretical trend is confirmed by the experiments, even if some discrepancies exist. (e) Results of dynamic tests conducted by applying repeated voltage steps to the finger ($R = 30$ mm). (f) Validation of the zipping model with a small mass ($P = 1$ g) applied at the finger tip.

model and experiments is reduced. The no zip voltage shows a very good matching, while the full zip voltage shows a 40% error (compared to over 200% for the copper case). The error reduction compared to the copper coating can be due to (1) controlling for surface, (2) electrical effects not modeled mediated by the presence of the paper layer.

Time response of both zipping and unzipping is very important for the use of EA in soft grippers. We conducted dynamic tests by applying repeated voltage steps (3 s on and 3 s off, increased by 400 V at each cycle). Results of zipping time at different voltages are shown in Fig. 5e and zipping and unzipping cycles in Supplementary Section S2. For the highest used voltage (3.6 kV) we measure a 90%-time response for zipping of 0.419 s and for unzipping of 0.328 s (see also Supplementary video 3).

Finally, we conducted an experiment of EA zipping with load lifting (Fig. 5f). We attached a small load (1 g) to the finger tip (see Supplementary Section S3) and measured the zipping angle at different voltages. The V no zip value is unchanged compared to the case without the load, as expected from (9) since it is dominated by the bending energy of the finger. On the contrary, the V full zip value increases significantly, becoming higher than the value that is safe to apply to the EA finger (4 kV). V full zip is affected by the gravitational energy, which increases due to the added load. Model and experiments show a very good agreement.

5. Conclusions

This work deals with EA soft grippers passively wrapping curved objects by means of EA-induced zipping (EAZ). We presented an analytical model (with two alternative approaches) to describe the zipping process, and experiments to test the model outcomes. The model shows that EAZ on curved objects is the result of the balance between electrical and mechanical features of the system. Two voltage thresholds dictate the EAZ phenomenon: we found that no wrapping appears until the applied voltage reaches the first threshold, and that full wrapping is only expected when a voltage greater than the second threshold is delivered by the voltage supplier. Between the two values, the wrapping angle increases with the applied voltage.

The model results are in good agreement with experiments, even if some observed phenomena need further investigation. The model does not account for the dynamics of the charges in the system or for the surface properties of the gripper-object interface, yet these effects seem to have a great influence in our experiments. Future investigations will focus on these issues.

Our model also provides design tools for the fabrication of improved passively wrapping EA soft grippers, highlighting the mutual relationship among electrical and mechanical parameters of the system and how it practically influences the wrapping behavior of the EA gripper.

The demonstrated wrapping capabilities promise very high holding force according to previous works [10,12]. However, extreme softness and compliance can still hinder manipulation capabilities of EA soft grippers, limiting their ability to rotate the grasped object or to move payloads fast. Future works will address this topic.

We believe that this work broadens the understanding of the capabilities of a passively conforming EA soft gripper, showing how wrapping moderately complex (curved) geometries can be obtained even without actuator-based conforming strategies. The outcomes shown in this work could also be adapted to various EAZ-based soft devices, such as HASELs [34], HAXELs [20], electro-ribbons and electro-origami [18] actuators, meaning that this paper can be used as a tool not only for the design of improved EA soft grippers, but also for soft actuators and soft machines that leverage Electroadhesion-induced Zipping.

Declaration of competing interest

The authors declare the following financial interests/personal relationships which may be considered as potential competing interests: Vito Cacucciolo reports equipment and supplies were provided by Omnigrasp SRL. Vito Cacucciolo reports a relationship with Omnigrasp SRL that includes: board membership and equity or stocks. Vito Cacucciolo has patent Electroadhesion-based shear gripping system and method of using there of pending to Ecole Polytechnique Fédérale de Lausanne (EPFL), Lausanne (CH).

Data availability

Data will be made available on request.

Acknowledgment

We thank Prof. Rocco Vertechy for providing us the P(VDF-TrFE-CTFE) films we used in our characterization. We acknowledge support by the following sources. The Italian Ministry of Education, University and Research under the Programme "Department of Excellence" Legge 232/2016 (Grant No. CUP - D94I18000260001)". The European Union - NextGenerationEU (National Sustainable Mobility Center CN00000023, Italian Ministry of University and Research Decree n. 1033 - 17/06/2022, Spoke 11 - Innovative Materials & Lightweighting). The European Union's Horizon Europe research and innovation program under grant agreement No 101092100. The opinions expressed are those of the authors only and should not be considered as representative of the European Union or the European Commission's official position. Neither the European Union nor the European Commission can be held responsible for them.

Appendix A. Supplementary data

Supplementary material related to this article can be found online at https://doi.org/10.1016/j.eml.2023.101999.

References

[1] J. Shintake, V. Cacucciolo, D. Floreano, H. Shea, Soft robotic grippers, Adv. Mater. 30 (2018) 1707035, http://dx.doi.org/10.1002/adma.201707035.

[2] J. Shintake, S. Rosset, B. Schubert, D. Floreano, H. Shea, Versatile soft grippers with intrinsic electroadhesion based on multifunctional polymer actuators, Adv. Mater. 28 (2016) 231–238, http://dx.doi.org/10.1002/adma.201504264.

[3] R. Chen, Z. Zhang, J. Guo, F. Liu, J. Leng, J. Rossiter, Variable stiffness electroadhesion and compliant electroadhesive grippers, Soft Robot. (2021) http://dx.doi.org/10.1089/soro.2021.0083, soro.2021.0083.

[4] V. Alizadehyazdi, M. Bonthron, M. Spenko, An electrostatic/gecko-inspired adhesives soft robotic gripper, IEEE Robot. Autom. Lett. 5 (2020) 4679–4686, http://dx.doi.org/10.1109/LRA.2020.3003773.

[5] E.W. Schaler, D. Ruffatto, P. Glick, V. White, A. Parness, An electrostatic gripper for flexible objects, in: 2017 IEEE/RSJ International Conference on Intelligent Robots and Systems, IROS, IEEE, Vancouver, BC, 2017, pp. 1172–1179, http://dx.doi.org/10.1109/IROS.2017.8202289.

[6] G. Hwang, J. Park, D.S.D. Cortes, K. Hyeon, K.-U. Kyung, Electroadhesion-based high-payload soft gripper with mechanically strengthened structure, IEEE Trans. Ind. Electron. 69 (2022) 642–651, http://dx.doi.org/10.1109/TIE.2021.3053887.

[7] V. Cacucciolo, H. Shea, G. Carbone, Peeling in electroadhesion soft grippers, Extreme Mech. Lett. 50 (2022) 101529, http://dx.doi.org/10.1016/j.eml.2021.101529.

[8] K.M. Digumarti, V. Cacucciolo, H. Shea, Dexterous textile manipulation using electroadhesive fingers, in: 2021 IEEE/RSJ International Conference on Intelligent Robots and Systems, IROS, IEEE, Prague, Czech Republic, 2021, pp. 6104–6109, http://dx.doi.org/10.1109/IROS51168.2021.9636095.

[9] I.-D. Sîrbu, M. Bolignari, S. D'Avella, F. Damiani, L. Agostini, P. Tripicchio, R. Vertechy, L. Pancheri, M. Fontana, Adhesion state estimation for electrostatic gripper based on online capacitance measure, Actuators. 11 (2022) 283, http://dx.doi.org/10.3390/act11100283.

[10] V. Cacucciolo, J. Shintake, H. Shea, Delicate yet strong: Characterizing the electro-adhesion lifting force with a soft gripper, in: 2019 2nd IEEE International Conference on Soft Robotics (RoboSoft), IEEE, Seoul, Korea (South), 2019, pp. 108–113, http://dx.doi.org/10.1109/ROBOSOFT.2019.8722706.

[11] D.J. Levine, G.M. Iyer, R. Daelan Roosa, K.T. Turner, J.H. Pikul, A mechanics-based approach to realize high–force capacity electroadhesives for robots, Science Robotics 7 (2022) eabo2179, http://dx.doi.org/10.1126/scirobotics.abo2179.

[12] M. Mastrangelo, V. Cacucciolo, High-force soft grippers with electroadhesion on curved objects, in: 2022 IEEE 5th International Conference on Soft Robotics (RoboSoft), IEEE, Edinburgh, United Kingdom, 2022, pp. 384–389, http://dx.doi.org/10.1109/RoboSoft54090.2022.9762116.

[13] J. Guo, K. Elgeneidy, C. Xiang, N. Lohse, L. Justham, J. Rossiter, Soft pneumatic grippers embedded with stretchable electroadhesion, Smart Mater. Struct. 27 (2018) 055006, http://dx.doi.org/10.1088/1361-665X/aab579.

[14] B.N.J. Persson, General theory of electroadhesion, J. Phys.: Condens. Matter. 33 (2021) 435001, http://dx.doi.org/10.1088/1361-648X/abe797.

[15] G. Gu, J. Zou, R. Zhao, X. Zhao, X. Zhu, Soft wall-climbing robots, Sci. Robot. 3 (2018) 13, http://dx.doi.org/10.1126/scirobotics.aat2874.

[16] V. Ramachandran, J. Shintake, D. Floreano, All-fabric wearable electroadhesive clutch, Adv. Mater. Technol. 4 (2019) 1800313, http://dx.doi.org/10.1002/admt.201800313.

[17] R. Hinchet, H. Shea, High force density textile electrostatic clutch, Adv. Mater. Technol. 5 (2020) 1900895, http://dx.doi.org/10.1002/admt.201900895.

[18] M. Taghavi, T. Helps, J. Rossiter, Electro-ribbon actuators and electro-origami robots, Science Robotics 3 (2018) eaau9795, http://dx.doi.org/10.1126/scirobotics.aau9795.

[19] P. Rothemund, N. Kellaris, S.K. Mitchell, E. Acome, C. Keplinger, HASEL artificial muscles for a new generation of lifelike robots—Recent progress and future opportunities, Adv. Mater. 33 (2021) 2003375, http://dx.doi.org/10.1002/adma.202003375.
[20] E. Leroy, R. Hinchet, H. Shea, Multimode hydraulically amplified electrostatic actuators for wearable haptics, Adv. Mater. (2020) 2002564, http://dx.doi.org/10.1002/adma.202002564.
[21] L.K. Borden, A. Gargava, S.R. Raghavan, Reversible electroadhesion of hydrogels to animal tissues for suture-less repair of cuts or tears, Nature Commun. 12 (2021) 4419, http://dx.doi.org/10.1038/s41467-021-24022-x.
[22] R. Chen, R. Song, Z. Zhang, L. Bai, F. Liu, P. Jiang, D. Sindersberger, G.J. Monkman, J. Guo, Bio-inspired shape-adaptive soft robotic grippers augmented with electroadhesion functionality, Soft Robot. 6 (2019) 701–712, http://dx.doi.org/10.1089/soro.2018.0120.
[23] S. Park, K. Mondal, R.M. Treadway, V. Kumar, S. Ma, J.D. Holbery, M.D. Dickey, Silicones for stretchable and durable soft devices: Beyond sylgard-184, ACS Appl. Mater. Interfaces. 10 (2018) 11261–11268, http://dx.doi.org/10.1021/acsami.7b18394.
[24] Dow Corning, Sylgard 184 Silicone Elastomer datasheet., (n.d.). https://www.dow.com/documents/en-us/productdatasheet/11/11-31/11-3184-sylgard-184-elastomer.pdf.
[25] B. Behzadnezhad, B.D. Collick, N. Behdad, A.B. McMillan, Dielectric properties of 3D-printed materials for anatomy specific 3D-printed MRI coils, J. Magn. Reson. 289 (2018) 113–121, http://dx.doi.org/10.1016/j.jmr.2018.02.013.
[26] S. Simula, S. Ikäläinen, K. Niskanen, T. Varpula, H. Seppä, A. Paukku, Measurement of the Dielectric Properties of Paper, Vol. 43, 1999, p. 6.
[27] PolyK technologies, P(VDF-TrFE-CTFE) datasheet, High Dielectric Constant P(VDF-TrFE-CTFE) Terpolymer Film. (n.d.). https://piezopvdf.com/ctfe-terpolymer-film-low-ctfe-18-um/.
[28] G. Kofod, P. Sommer-Larsen, R. Kornbluh, R. Pelrine, Actuation response of polyacrylate dielectric elastomers, J. Intell. Mater. Syst. Struct. 14 (2003) 787–793, http://dx.doi.org/10.1177/104538903039260.
[29] F.B. Albuquerque, H. Shea, Influence of humidity, temperature and prestretch on the dielectric breakdown strength of silicone elastomer membranes for DEAs, Smart Mater. Struct. 29 (2020) 105024, http://dx.doi.org/10.1088/1361-665X/aba5e3.
[30] Z. Suo, Theory of dielectric elastomers, Acta Mech. Solida Sin. 23 (2010) 30, http://dx.doi.org/10.1016/S0894-9166(11)60004-9.
[31] E. Hajiesmaili, D.R. Clarke, Dielectric elastomer actuators, J. Appl. Phys. 129 (2021) 151102, http://dx.doi.org/10.1063/5.0043959.
[32] M. Righi, M. Fontana, R. Vertechy, M. Duranti, G. Moretti, Analysis of dielectric fluid transducers, in: Y. Bar-Cohen (Ed.), Electroactive Polymer Actuators and Devices (EAPAD) XX, SPIE, Denver, United States, 2018, p. 29, http://dx.doi.org/10.1117/12.2297082.
[33] N. Kellaris, V.G. Venkata, P. Rothemund, C. Keplinger, An analytical model for the design of peano-HASEL actuators with drastically improved performance, Extreme Mech. Lett. 29 (2019) 100449, http://dx.doi.org/10.1016/j.eml.2019.100449.
[34] E. Acome, S.K. Mitchell, T.G. Morrissey, M.B. Emmett, C. Benjamin, M. King, M. Radakovitz, C. Keplinger, Hydraulically amplified self-healing electrostatic actuators with muscle-like performance, Science 359 (2018) 61–65, http://dx.doi.org/10.1126/science.aao6139.